tvst

Article

Optical Coherence Tomography Angiography in Macular Neovascularization: A Comparison Between Different OCTA Devices

Rodolfo Mastropasqua[1], Federica Evangelista[2], Francesco Amodei[2], Rossella D'Aloisio[2], Filomena Pinto[2], Emanuele Doronzo[2], Pasquale Viggiano[2], Annamaria Porreca[3], Marta Di Nicola[3], Mariacristina Parravano[4], and Lisa Toto[2]

[1] Institute of Ophthalmology, University of Modena and Reggio Emilia, Modena, Italy
[2] Ophthalmic Clinic, Department of Medicine and Science of Ageing, University G. D'Annunzio Chieti-Pescara, Chieti, Italy
[3] Department of Economic Studies, University "G. D'Annunzio" Chieti-Pescara, Chieti, Italy
[4] IRCCS – Fondazione Bietti, Rome, Italy

Correspondence: Federica Evangelista, Ophthalmic Clinic, Department of Medicine and Science of Ageing, University G. D'Annunzio Chieti Pescara, via dei Vestini 31, 66100, Chieti, Italy. e-mail: federica.evan@hotmail.com

Received: June 13, 2020
Accepted: August 16, 2020
Published: October 7, 2020

Keywords: macular neovascularization; optical coherence tomography; swept source OCTA

Citation: Mastropasqua R, Evangelista F, Amodei F, D'Aloisio R, Pinto F, Doronzo E, Viggiano P, Porreca A, Di Nicola M, Parravano M, Toto L. Optical coherence tomography angiography in macular neovascularization: A comparison between different OCTA devices. Trans Vis Sci Tech. 2020;9(11):6, https://doi.org/10.1167/tvst.9.11.6

Purpose: The purpose of this study is to compare the ability of 3 optical coherence tomography angiography (OCTA) devices to measure lesion area in patients with macular neovascularization (MNV) with type 1, 2 and mixed neovascularization (NV).

Methods: OCTA, fluorescein angiography (FA), indocyanine green angiography (ICGA), and structural optical coherence tomography (OCT) were performed. NV lesion area measurements were performed by two graders.

Results: Twenty-eight eyes were included: 20 with NV were classified as type 1, 6 as type 2, and 2 as mixed type. AngioVue and Spectralis detected the NV in 26 out of 28 eyes (92.8%). The intraclass correlation coefficient (ICC) between readers for the three different OCTA with the different slabs was high. The NV area was larger in the outer retina to choriocapillaris (ORCC) and choriocapillaris (CC) images for the AngioVue device and the PLEX Elite device compared to avascular images ($P < 0.05$). The mean values of the NV area were not significantly different among the three instruments (Friedman test, $P > 0.05$) for the avascular zone (AV), ORCC, and CC images. Median (interquartile range [IQR]) NV were significantly different among avascular images, ORCC images, and CC images of the AngioVue device ($P = 0.046$), of the Spectralis device ($P = 0.015$), and the PLEX Elite device ($P < 0.001$).

Conclusions: The ORCC slabs showed the highest detection rate for NV detection independently to the device used, and swept source (SS)-OCTA measurements of ORCC slabs showed the highest detection rate of NVs compared to the spectral domain (SD)-OCTA.

Translational Relevance: It is pivotal to realize how much we can rely on OCTA to make a diagnosis of NV.

Introduction

Optical coherence tomography angiography (OCTA) is a quick and noninvasive[1] diagnostic examination that provides qualitative and the quantitative blood flow information of the retinal and choroidal circulation. In particular, OCTA has recently been used for the diagnosis and follow-up of macular neovascularization (MNV).[2] MNV indicates a neovascular age-related macular degeneration (AMD) with neovascularization (NV) that does not necessarily originate from the choroid, being an invasion by vascular and associated tissues into the outer retina, subretinal space, or subretinal pigment epithelium (sub-RPE) space in varying combinations. The anatomic location of the NV determined by optical coherence tomography (OCT) imaging is used to subclassify the vascular

component of the disease process. Type 1 NV is applied when the vessels originate from the choroid and remain under the RPE. Polypoidal choroidal vasculopathy is an important subtype of NV defined by a branching vascular network and nodular vascular agglomerations. Type 2 NV is denoted if NV that originates in the choroid breaks through the RPE to reach the subretinal space. Type 3 NV is to be used when the vascular complex originates in the retina. If prominent NV is present in the subretinal and sub-RPE compartments, the term mixed type 1 and type 2 NV can be applied. Fluorescein angiography (FA) and indocyanine green angiography (ICGA) have traditionally been considered the gold standard for clinical assessment of MNV.[3,6,7] Undoubtedly one of the major advantages of OCTA compared with FA and ICGA is the absence of dye injection, which allows us to visualize better the structure and the area of vessels. Even though dye administration is generally safe in patients, serious allergic reactions may occur, and these techniques are considered invasive and require considerable patient cooperation. On the contrary, OCTA provides noninvasive assessment of the retinal and choroidal vasculatures.[1] Moreover, OCTA has the additional advantage of depth resolution with improved visualization of the deeper vascular plexuses. Compared to spectral domain OCTA (SD-OCTA) using a wavelength at approximately 840 nm, the latest generation of swept source OCTA (SS-OCTA) has significantly improved our capability to investigate the choriocapillaris (CC) thanks to the highest velocity of scan acquisition (400,000 A-scans/second), and the use of a longer wavelength (approximately 1050 nm wavelength), which better penetrates deeper tissues and is less scattered by the RPE. This allows an improved visualization of the choroid both on cross-sectional as well as en face OCTA imaging,[6] and may also improve visualization of MNV, especially the sub-RPE component of the membrane.

The aim of this study was to evaluate the sensibility and accuracy of different OCTA devices in detecting treatment-naïve MNV eyes.

Materials and Methods

Study Participants

In this prospective observational study, 28 eyes of 28 subjects (18 men and 10 women) aged between 58 and 83 years old with treatment-naïve MNV were enrolled at the ophthalmology clinic of University "G. d'Annunzio", Chieti-Pescara, Italy, between June 2018 and January 2019. All patients enrolled were imaged by three different OCTA devices. FA and ICGA were performed at the same visit in all patients. Criteria for inclusion were: age > 50 years old; and presence of dye angiography detectable MNV. The exclusion criteria were: (1) any previous ocular surgery (including intravitreal injections); (2) laser treatments; (3) history of glaucoma; (4) vascular retinal diseases; and (5) medium lens opacities (according to the Lens Opacities Classification System).

Imaging

Patients underwent OCTA imaging using both SD-OCTA and SS-OCTA devices. SD-OCTA was performed using (i) RTVue XR Avanti SD-OCT device with AngioVue software (version 2018.1.0.24; Optovue, Inc., Freemont, CA, USA), which is based on a split spectrum amplitude decorrelation angiography (SSADA) algorithm and (ii) Spectralis HRA-OCTA (version 6.12.4.0; Heidelberg Engineering, Heidelberg, Germany) based on a full-spectrum amplitude-decorrelation angiography (FSADA) with a probabilistic approach to generate high-contrast almost binarized appearance OCTA images. These instruments have an axial resolution of approximately 3 µm and a transverse resolution of approximately 6 µm.

On the other side, SS-OCTA images were acquired with PLEX Elite 9000 device (version 1.7.0.27959; Carl Zeiss Meditec, Inc., Dublin, CA, USA) using a swept laser source with a central wavelength of 1050 nm and operating at 100,000 A scans per second. This instrument has an axial resolution of approximately 5 µm and a lateral resolution estimated at approximately 14 µm. The dataset was processed using the complex optical microangiography (OMAG^{C}) algorithm to generate the angiographic signals.[7–9] Poor quality images with a signal strength index (SSI) less than six or significant motion artifacts were not included.

In order to assure maximum image resolution and coverage of the entire lesion, 3 × 3 mm volumes were used for OCTA comparison. Only 2 NVs needed 6 × 6 mm scans to cover the entire lesion (Fig. 1).

Characteristic's details of each used scans are shown in Table 1.

The same segmentation and image processing strategies were applied to both the SD-OCTA and SS-OCTA datasets.

For the Plex Elite device, a fully automated segmentation algorithm was used for the three-dimensional structural OCT data and applied to OCTA flow intensity with sum projection analyses, to obtain three different OCTA en face images: (1) the outer retina to choriocapillaris (ORCC) image that was obtained with a slab extended from the outer boundary of the outer

Table 1. Optical Coherence Tomography Angiography Instruments

System	AngioVue	Spectralis OCTA	PLEX Elite 9000
Manufactor	OptoVue, Fremont Inc., CA, USA	Heidelberg Engineering, Heidelberg, Germany	Carl Zeiss Meditec Inc., Dublin, CA, USA
OCT device	RTVue XR Avanti SD-OCT	OCT2 SD-OCT	PLEX Elite 9000 SS-OCT
Software version	2018.1.0.24	6.12.4.0	1.7.0.27959
Algorithm	SSADA	FSADA probabilistic approach	OMAG^{C}
Wavelength (nm)	840	870	1050
Scan speed (A-scan/s)	70,000	85,000	100,000
A-scan count (3 × 3)	304 × 304	512 × 512	300 × 300
A-scan count (6 × 6)	400 × 400	512 × 512	500 × 500
Eye-tracking technology	DualTrac	SMARTTrack	FastTrac

FSADA, full-spectrum amplitude-decorrelation angiography; OMAGC, optical microangiography complex; SSADA, split-spectrum amplitude decorrelation algorithm.

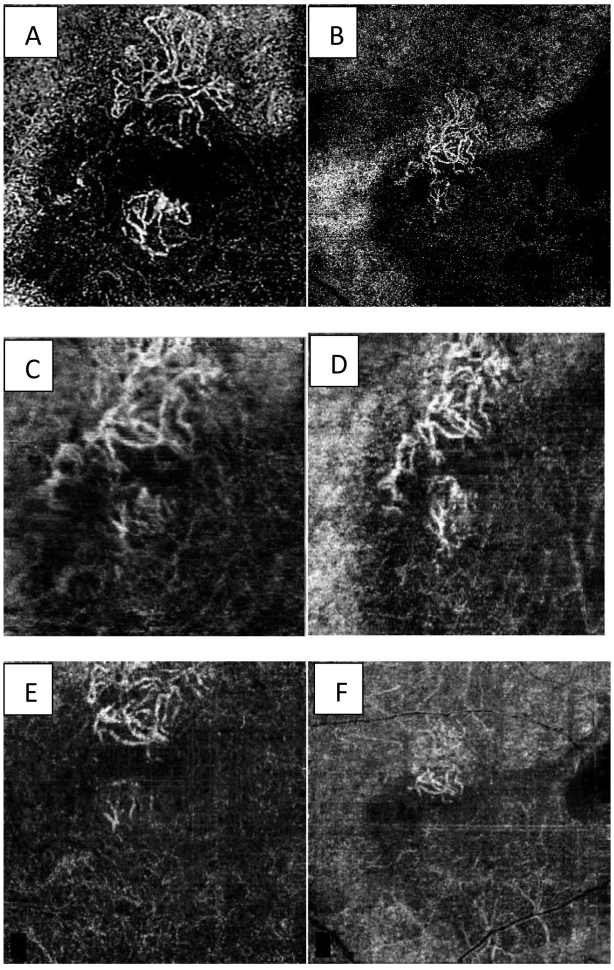

Figure 1. En face SS and SD-OCTA images from the left eye of a 72-year-old man with macular neovascular disease. All images were obtained using the outer retina to choriocapillaris (ORCC) image. (**A**) PlexElite OCTA 3 × 3-mm^2 scan. (**B**) PlexElite OCTA 6 × 6-mm^2. (**C**) Spectralis OCTA 3 × 3-mm^2 scan. (**D**) Spectralis OCTA 6 × 6-mm^2 scan. (**E**) Optovue OCTA 3 × 3-mm^2 scan. (**F**) Optovue OCTA 6 × 6-mm^2.

plexiform layer (OPL) to 8 µm beneath Bruch's membrane, (2) the avascular zone (AV) that was obtained using a slab, which was comprised from the outer boundary of the OPL to 99 µm above Bruch's membrane, and (3) the CC image obtained using a slab 20 µm thick starting from Bruch's membrane.

Regarding the SD-OCTA devices, fully automated segmentation algorithms and projection artifact removal algorithms were used. The avascular slab and CC slab were obtained using the default layer segmentation settings of the device, on the contrary, the ORCC segmentation was set manually.

This ORCC slab has been shown to be useful for visualizing important features of type I and type II choroidal neovascularization (CNV).[10]

The images of all devices were exported from each device as JPEG files with a resolution different per each device, and then normalized and analyzed.

Image Processing

The main outcome measure was the flow area within the neovascular lesion.

Image processing was performed with ImageJ software version 1.52a (National Institutes of Health, Bethesda, MD, USA; available at http://rsb.info.nih.gov/ij/index.html; Fig. 2).

In brief, the NV lesion was manually circumscribed on each en face image, as described above, by two independent experienced readers (F.A. and F.E.) and the flow within this area was computed as the number of pixels over a nonperfusion (or noise) threshold. Notably, a pixel-mm scale was set to obtain a converted and comparable mm^2 area value.

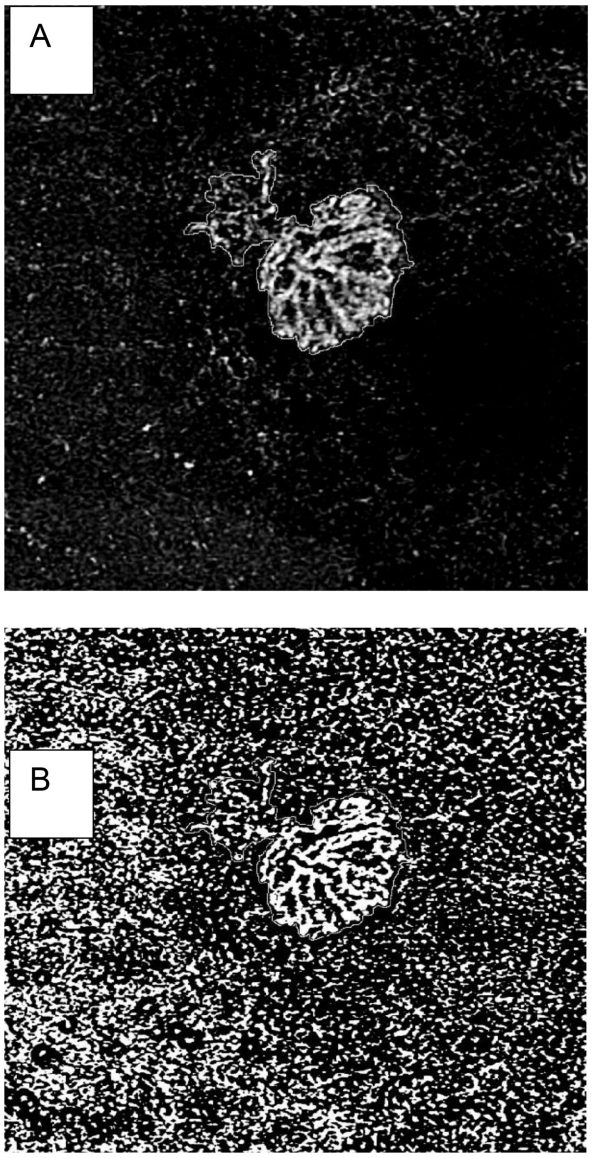

Figure 2. Image processing: in the acquired avascular en face image, the NV lesion was manually delineated by two independent experienced readers. (**A**) The binarized image (**B**) was then computed and analyzed.

Statistical Analysis

Qualitative variables were presented as frequency and percentage. Continuous variables were tested for normal distribution with Shapiro-Wilk's test and reported as the median and interquartile range (IQR). Results were reported separately for each device.

Lin's concordance correlation coefficient (CCC) with the 95% confidence intervals was calculated to assess the interobserver reproducibility of measurements. To each patient, the mean values considering observer one and two were attributed.

The Friedman test was applied independently to evaluate the significant differences among the devices and the slabs.

All tests were two-sided, and a level of statistical significance was set at $P < 0.05$. All the statistical analyses were performed using R software environment for statistical computing and graphics version 3.5.2 (R Foundation for Statistical Computing, Vienna, Austria; https://www.R-project.org/).

Results

Characteristics of Patients and NV Included in the Analysis

The number of included patients was 28 (18 men and 10 women) with a mean age of 72.2 ± 6.9 years. All 28 eyes with treatment-naïve MNV who fulfilled the inclusion and exclusion criteria were included in the analysis. The patients' distribution is the following: 20 (71.4%) had type 1 NV, 6 (21.4%) had type 2 NV, and 2 (7.1%) had mixed types 1 and 2 NV. Ophthalmoscopy and multicolor image did not show retinal and subretinal hemorrhages causing shadowing effects or reducing the signal strength of the OCT scan.

Twenty-six MNVs of 28 MNVs were visible for the complete lesion extension using 3 × 3 mm volumes scans both with SD-OCTA and SS-OCTA devices; whereas 2 of 28 MNVs, which were not completely visualized for the entire lesion extension with the 3 × 3 mm scan, were scanned both with 3 × 3 mm and 6 × 6 mm scans using the 3 devices.

Detection Rate

In our series, only 1 of 3 OCTA devices detected the NV in 100% of eyes on en face images.

AngioVue and Spectralis detected the NV in 26 of 28 eyes (92.8%), not displaying 2 quite small type 1 NVs (mean measured flow area 0.053 and 0.111 mm^2, respectively) using any type of segmentation. Notably, the presence of all NVs was detectable on angio B scan (Fig. 3).

For the AngioVue device, the avascular slab showed 24 of 28 (85.7%) NVs; and the ORCC slab and CC slab showed 26 of 28 (92.8%) NVs.

For the Spectralis device, the avascular slab and the ORCC slab showed 26 of 28 (92.8%) NVs, and the CC slab showed 24 of 28 (85.7%) NVs.

For the PLEX Elite device, the avascular slab showed 20 of 28 (71.4%) NVs, the ORCC slab showed 28 of 28 (100%) NVs, and the CC slab showed 24 of 28 (85.7%) NVs.

Table 2. Friedman Test Comparison of Measurements From Three OCTA Images in the Neovascularization Cohort

	AV	ORCC	CC	*P Value*
ANGIOVUE	0.160 (0.017–0.441)	0.268 (0.053–0.631)	0.236 (0.058–0.745)	***0.046***
PLEX-ELITE	0.039 (0–0.284)	0.519 (0.083–0.98)	0.529 (0.058–0.941)	***< 0.001***
SPECTRALIS	0.258 (0.143–0.701)	0.258 (0.143–0.701)	0.215 (0.018–0.542)	***0.015***
P value	***0.050***	***0.607***	***0.223***	

NV area, mm^2, median (IQR).

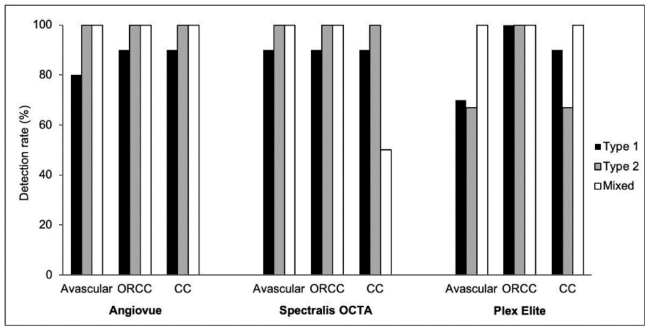

Figure 3. Detection rate for type 1, type 2 and mixed type 1 and 2 of MNV for the different slabs in each device.

Inter Reader Agreement

The intraclass correlation coefficient (ICC) between readers for the three different OCTA devices was 0.970 (95% confidence interval [CI] = 0.909–0.990) for the AV image, 0.994 (95% CI = 0.981–0.998) for the ORCC image, and 0.996 (95% CI = 0.988–0.999) for the CC image of the AngioVue device, 0.996 (95% CI = 0.988–0.999) for the AV image, 0.996 (95% CI = 0.988–0.999) for the ORCC image, and 0.991 (95% CI = 0.972–0.997) for the CC image of the Spectralis device, 0.968 (95% CI = 0.902–0.989) for the AV image, 0.993 (95% CI = 0.978–0.998) for the ORCC image, and 0.987 (95% CI = 0.959–0.996) for the CC image of the PLEX Elite device. These ICC values indicate good agreement between the two readers.

Inter Modality Comparison

The mean values of the NV area were not significantly different among the three instruments (Friedman test, $P > 0.05$) for the AV, ORCC, and CC images (Table 2).

Median (IQR) NV were significantly different among the avascular image, the ORCC image, and the CC image of the AngioVue device ($P = 0.046$), of the Spectralis device ($P = 0.015$), and the PLEX Elite device ($P < 0.001$).

Median and IQR areas were 0.160 (IQR = 0.017–0.441) for the avascular image, 0.268 (IQR = 0.053–0.631) for the ORCC image, and 0.236 (IQR = 0.058–0.745) for the CC image of the AngioVue device; 0.258 (IQR = 0.143–0.701) for the AV image, 0.258 (IQR = 0.143–0.701) for the ORCC image, and 0.215 (IQR = 0.018—0.542) for the CC image of the Spectralis device; 0.039 (IQR = 0.0–0.284) for the AV image, 0.519 (IQR = 0.083–0.980) for the ORCC image, and 0.529 (IQR = 0.058–0.941) for the CC image of the PLEX Elite device.

The NV area was larger in the ORCC and CC images for the AngioVue device and the PLEX Elite device compared to avascular images ($P < 0.05$).

Discussion

OCTA is a new imaging technique that uses motion contrast imaging to high-resolution volumetric blood flow information generating angiographic images in a matter of seconds.[11]

The recent literature focused on the capability of OCTA to identify MNV compared to traditional angiographic imaging and the sensitivity and specificity of OCTA in detecting neovascular lesion1.[5–17]

Costanzo et al.[14] detected a smaller size of MNV using OCTA compared to ICGA both in the intermediate and late phases, possibly related to leakage of the dye on late phase of the examination. Corvi et al.[12] compared four different OCTA device measurements with early ICGA images. The mean values of MNV were significantly different between SD and SS-OCTA devices and the MNV area was significantly larger with ICGA. They argued that the detected differences between OCTA devices was related to the use of different slabs for each device and the presence of projection artifacts. Before this study, the prototype Spectralis OCTA was the closest to ICGA measuring the MNV area. This result is in contrast with previous studies comparing SS-OCTA and SD-OCTA.[15,16]

Miller et al.[15] showed that a prototype SS-OCTA device was more accurate compared to a SD-OCTA device to measure the lesion area of MNV. According to the authors, SS-OCTA results were related to

the longer wavelength and reduced optical scattering and absorption from the retinal pigment epithelium complex.

In the same way Novais et al.[17] demonstrated that SS-OCTA defined better the full extent of MNV vasculature compared with SD-OCTA.

Our results indicate that SS-OCTA imaging provided a more accurate representation of the MNV compared with SD-OCTA, in particular the SS-OCTA measurements showed the highest detection rate of NVs with ORCC slab and the larger NV area in ORCC and CC slabs compared to the other two OCTA devices with all the different segmentations.

Considering the detection rate of MNV, the avascular segmentation showed the lowest value compared with other segmentations and this was hypothesized to be secondary to the limited capability of this slab to incorporate the whole NV lesion, which may be due to prevalence of type 1 NV lesions in the sample. This was particularly evident with the Angiovue and the Plex Elite devices (detection rate of 85.7% and 71.4%, respectively), in fact, the avascular slab of the PLEX Elite extends up to the inner segment/outer segment (IS/OS) junction. On the contrary, the high detection rate of the Spectralis device is due to the larger extension of the avascular slab extending up to the Bruch's membrane.

ORCC slabs showed the highest detection rate for NV visualization independently to the device used being 92.8% with both SD-OCTA devices and 100% with the PLEX Elite device.

Considering the lesion area, ORCC and CC slabs either with the Angiovue device or the PLEX Elite device detected larger measurements compared to avascular slabs, showing the PLEX Elite device had the highest values of the lesion area (0.519 and 0.529 mm^2 with ORCC and CC slab, respectively). These results are in agreement with our interpretation that ORCC and CC segmentation better incorporate the type 1 NVs prevalent in our sample.

Our results showed an excellent overall inter-reader agreement for all slab of the three devices.

Parravano et al.[18] showed that en face images obtained using the ORCC and RPE-RPE fit slabs with the PLEX Elite device allowed an accurate and reproducible quantification of the MNV area compared to the CC slabs.

Our results agree with the data from the literature confirming the greater accuracy of SS-OCTA in detecting MNV compared to SD-OCTA. Moreover, ORCC slabs of the PLEX Elite provides the highest detection rate and the visualization of the greatest lesion extension in our study.

Our results partially disagree with Corvi et al.[12] who found a better capability of the Spectralis device compared to the PLEX Elite device in identifying NV lesions size using ORCC slabs with a lesion area measurement that was the closest to the ICGA measured area. They argued that this was related to the highest number of A-scan per B-scan of the Spectralis OCTA.

A detailed detection of the MNV presence and lesion extension using OCTA is mandatory to diagnose and monitor the disease. The identification of the more sensitive and specific device would translate into less use of the FA for the diagnosis and monitoring of MNV. It means less costs for the health system and less waiting for treatment. Despite the superiority of the SS-OCTA, the ability of the SD-OCTA is not to be underestimated because, with the right experience of the clinician and support of the structural OCT, also the SD-OCTA achieves a good diagnostic sensitivity.

Overall, we observed that ORCC and CC images provided an accurate and reproducible quantification of NV lesions for any device.

Unfortunately, one of the main limitations in our study was the small number of patients included, which reduces the power of our analysis, and consequently the potential of a specific slab to evaluate MNV.

Second, we used 3 × 3 mm images resulting from a number of A-scan (hence pixel) different per each device, this may lead to a different distance between each scan and consequently a different detection and representation of the MNV flow.

Finally, image quality may have impacted on perfusion measurements. However, poor quality images or significant motion artifacts were not included in our analysis.

In summary, OCTA both with SD or SS technology using different segmentation strategies allowed an accurate and reproducible quantification of MNV lesion. In particular, ORCC slabs showed the highest detection rate for NV detection independently to the device used, and SS-OCTA measurements of ORCC slabs showed the highest detection rate of NVs compared to the SD-OCTA.

Acknowledgments

Disclosure: **R. Mastropasqua,** None; **F. Evangelista,** None; **F. Amodei,** None; **R. D'Aloisio,** None; **F. Pinto,** None; **E. Doronzo,** None; **P. Viggiano,** None; **A. Porreca,** None; **M. Di Nicola,** None; **M. Parravano,** None; **L. Toto,** None

References

1. Jia Y, Tan O, Tokayer J, et al. Split-spectrum amplitude-decorrelation angiography with optical coherence tomography. *Opt Express*. 2012;20:4710–4725.
2. Spaide RF, Jaffe GJ, Sarraf D, et al. Consensus nomenclature for reporting neovascular age-related macular degeneration data consensus on neovascular age-related macular degeneration nomenclature study group. *Ophthalmology*. 2020;127:616–636.
3. Kotsolis AI, Killian FA, Ladas ID, Yannuzzi LA. Fluorescein angiography and optical coherence tomography concordance for choroidal neovascularisation in multifocal choroidtis. *Br J Ophthalmol*. 2010;94:1506–1508.
4. Stanga PE, Lim JI, Hamilton P. Indocyanine green angiography in chorioretinal diseases: Indications and interpretation: an evidence-based update. *Ophthalmology*. 2003;110:15–21; quiz 22–23.
5. Do DV. Detection of new-onset choroidal neovascularization. *Curr Opin Ophthalmol*. 2013;24:244–247.
6. Choi W, Waheed NK, Moult EM, Adhi M, Duker JS, Fujimoto JG. Ultrahigh speed swept source optical coherence tomography angiography of retinal and choriocapillaris alterations in diabetic patients with and without retinopathy. HHS Public Access. *Retina (Philadelphia, PA)*. 2018;37(May 2014):11–21.
7. Wang RK, An L, Francis P, Wilson DJ. Depth-resolved imaging of capillary networks in retina and choroid using ultrahigh sensitive optical microangiography. *Opt Lett*. 2010;35:1467.
8. An L, Subhush HM, Wilson DJ, Wang RK. High-resolution wide-field imaging of retinal and choroidal blood perfusion with optical microangiography. *J Biomed Opt*. 2010;15:026011.
9. Huang Y, Zhang Q, Thorell MR, et al. Swept-source OCT angiography of the retinal vasculature using intensity differentiation-based optical microangiography algorithms. *Ophthalmic Surg Lasers Imaging Retin*. 2014;45:382–389.
10. Moult E, Choi W, Waheed NK, et al. Ultrahigh-speed swept-source OCT angiography in exudative AMD. HHS Public Access. *Ophthalmic Surg Lasers Imaging Retina*. 2014;45:496–505.
11. deCarlo TE, A Romano, Waheed NK, Duker JS. A review of optical coherence tomography angiography (OCTA). *Int J Retina Vitreous*. 2015;1:15.
12. Corvi F, Cozzi M, Barbolini E, et al. Comparison between several optical coherence tomography angiography devices and indocyanine green angiography of choroidal neovascularization. *Retina*. 2020;40:873–880.
13. Told R, Sacu S, Hecht A, et al. Comparison of SD-optical coherence tomography angiography and indocyanine green angiography in type 1 and 2 neovascular age-related macular degeneration. *Investig Ophthalmol Vis Sci*. 2018;59:2393–2400.
14. Costanzo E, Miere A, Querques G, Capuano V, Jung C, Souied EH. Type 1 choroidal neovascularization lesion size: Indocyanine green angiography versus optical coherence tomography angiography. *Investig Ophthalmol Vis Sci*. 2016;57:OCT307–OCT313.
15. Miller AR, Roisman L, Zhang Q, et al. Comparison between spectral-domain and swept-source optical coherence tomography angiographic imaging of choroidal neovascularization. *Invest Ophthalmol Vis Sci*. 2017;58:1499–1505.
16. Zhang Q, Chen C, Chu Z, et al. Automated quantitation of choroidal neovascularization : a comparison study between spectral-domain and swept-source OCT angiograms. *Invest Ophthalmol Vis Sci*. 2017;58:1506–1513.
17. Novais EA, Adhi M, Moult EM, et al. Choroidal neovascularization analyzed on ultrahigh-speed swept-source optical coherence tomography angiography compared to spectral-domain optical coherence tomography angiography. HHS Public Access. *Am J Ophthalmol*. 2016;164:80–88.
18. Parravano M, Borrelli E, Sacconi R, et al. A comparison among different automatically segmented slabs to assess neovascular AMD using swept source OCT angiography. *Transl Vis Sci Technol*. 2019;8:8.